ORIGINAL PAPER

Preparation and Properties of Biodegradable Poly(lactic acid)/Poly(butylene adipate-*co*-terephthalate) Blend with Epoxy-Functional Styrene Acrylic Copolymer as Reactive Agent

Naiwen Zhang · Chao Zeng · Liang Wang · Jie Ren

Abstract Poly (lactic acid) (PLA) and poly (butylene adipate-co-terephthalate) (PBAT) are biodegradable polyesters and can be blended by twin-screw extrusion. Epoxy-functional styrene acrylic copolymer (ESA) was used as reactive agent for PLA/PBAT blends and the mechanical properties, phase morphology, thermal properties, melt properties, and melt rheological behaviors of the blends were investigated. During thermal extrusion, ESA was mainly a chain extender for the PLA matrix but had no evident reaction with PBAT. The great improvement in the toughness of PLA based blends was achieved by the addition of PBAT of no less than 15 wt% and that of ESA of no more than 0.5 wt%. Although SEM micrographs and the reduced deviation of the terminal slope of G' and G'' indicated better compatibility and adhesion between the two phases, the blend with ESA was still a two-phase system as indicated in DSC curves. Rheological results reveal that the addition of ESA increased the storage modulus (G'), loss modulus (G'') and complex viscosity of the blend at nearly all frequencies. The melt strength and melt elasticity of the blend are improved by addition of ESA.

Keywords PLA · PBAT · ESA · Biodegradable · Reactive processing · Blend

N. Zhang · C. Zeng · L. Wang · J. Ren (✉)
Institute of Nano- and Bio-polymeric Materials, School of Material Science and Engineering, Tongji University, Cao'an Road 4800, Shanghai 200092, China
e-mail: renjie6598@163.com

J. Ren
Key Laboratory of Advanced Civil Engineering Materials, Ministry of Education, Tongji University, Shanghai 200092, China

Introduction

Development of consumer products from biodegradable and renewable materials is currently an area of great interest for researchers [1–5]. Poly(lactic acid) (PLA) is just one of those representative materials coming from renewable agricultural resources and can be decomposed into CO_2 and H_2O. PLA is a thermoplastic with high strength and high modulus, but its brittleness, thermal instability and low melt strength are critical for the manufacture of useful packaging products, such as sheet and film extrusion [6–8].

Poly (butylene adipate-co-terephthalate) (PBAT) is an aliphatic–aromatic copolymer, which is prepared by melt polycondensation of 1, 4-butanediol (BDO), dimethylterephthalate (DMT) and adipic acid with tetrabutylorthotitanate (TBOT) as the catalyst [9, 10]. Because of the flexibility and biodegradability, a commercial P (BA-co-44 mol % BT) with the trademark Ecoflex® was produced by BASF AG.

Various compatible and incompatible biodegradable polymer blends have been reported [11–14]. Consequently, combining the high toughness of PBAT and the high strength of PLA can result in a novel blend [15, 16]. The two fully biodegradable polymers have been considered as a complementary blender for each other. It has been studied that the elongation and toughness of PLA/PBAT blends increase dramatically with the increase of PBAT content (5–20 wt%) [17].

However, as a two-phase system, the incompatibility between PLA and PBAT, especially at interfaces, is still an unfavorable factor. Adding compatibilizer is a common method to improve the compatibility of blend. Compatibilizer in the blend tends to spread over the two-phase interface and then improves the compatibility significantly [18, 19]. Main influence of compatibilizer is to decrease the

interfacial tension between two phases and improve the stability and dispersible uniformity of disperse phase, and then make the incompatible blend into polymer alloy. Many reactive agents have been investigated and proved to be efficient for blends to improve the compatibility and performance [20]. An epoxy-multifunctional styrene acrylic copolymer (abbreviated as ESA) may be useful for reactive processing of PLA/PBAT blend. The heat and high shear stress in twin-screw extrusion might result in the cleavage of ester bonds of PLA or PBAT, and then the involved carboxyl and hydroxyl groups might react with epoxy groups of ESA [21, 22]. The weight average molecular weight (M_w) of ESA is 6,800 g/mol, and the epoxy equivalent weight is 285 g/mol.

In this paper, PBAT was blended into PLA to improve the toughness of PLA and ESA was used as reactive agent for compatibility. Then, the mechanical properties, phase morphology, thermal properties, melt properties and rheology of the PLA/PBAT blend were investigated.

Experimental

Materials

Pellets of PLA (M_w = 130,000 g/mol, polydispersity is about 1.7, and L-content is about 94 %, Tongjieliang Biomaterials Co., Ltd., Shanghai, China.), pellets of PBAT (M_w = 145,000 g/mol, polydispersity is about 2.6, Eco-flex®, BASF Corp.), and ESA (M_w = 6,800 g/mol, Epoxy equivalent weight = 285 g/mol, JONCRYL, BASF Corp.) were used without further purification.

Preparation of PLA/PBAT Blends with ESA

The blends were melt-blended using a co-rotating twin-screw extruder (LEISTRITZ Inc. Germany). The length-diameter ratio of screw is 41, and there are eleven heating zones, which can be controlled independently. The blend entered the extruder at zone 1 and exited at zone 11. Then the blend strips were cooled through flume and cut into pellets by dicing cutter. The zone temperatures were orderly set as 160, 165, 175, 190, 200, 210, 210, 185, 180, 175 and 170 °C. The test specimens were prepared from the extruded blends by using an injection molding machine (JETMASTER JN55-E) with a nozzle at 170 °C. The temperature of the mold was 25 °C and the cycle time was approximately 50 s.

Characterization

Charpy impact tests were conducted by using a ZBC1400-2 impact tester (Sans Group Company) adapted to the standard

ISO 179-2003. Tests were done on specimens of 80 mm × 10 mm × 4 mm and a pendulum of 4 J. Five replicates were tested for each sample to get an average value.

Tensile tests were conducted by using a CMT5105 electromechanical universal testing machine (Sans Group Company) adapted to the standard ISO 527-1993. The crosshead speed was 20 mm/min.

The intrinsic viscosities of PLA and PBAT were determined by using NCY series automatic viscometer with a solvent mixture of phenol and tetrachloroethane (equal weight proportion) at 25 °C.

The phase morphology was investigated by scanning electron microscopy (SEM, Hitachi S-2360N). Fracture-frozen cross sections of the impact test specimens of blends, taken either in a longitudinal or transverse direction, were coated with gold and observed under SEM at an accelerating voltage of 15 kV.

Thermal analysis data was performed using differential scanning calorimetry (DSC, Q100, TA instruments, USA). All specimens cut from pellets of different blends were tested under nitrogen atmosphere. In this study, DSC measurements were carried out by heating from −50 to 200 °C at a rate of 10 °C/min. DSC studies reveal the significant thermal properties of the samples, such as glass transition temperature (T_g), crystallizing point (T_c), crystallinity enthalpy change (ΔH_c), melting point (T_m) and melting enthalpy change (ΔH_m). The T_g was taken as the midpoint of the inflection, and the T_c and T_m were the peak temperatures of the crystallization exotherms and the melting endotherms.

The melt index (MFI, g/10 min) was measured using a RL-Z1B melt flow indexer at standard conditions of 190 °C and 2.16 kg nominal load.

Melt Strength (MS, Pa s) of the PLA/PBAT film was calculated by the following formula:

$$MS = \frac{8.5 \times 10^2 \Delta l * r_0^2}{MFI}$$

Δl is the length of the extruded polymer as the diameter of that reduced by 50 %, r_0 is the initial radius of the extruded polymer, MFI is the melt index value.

Rheological behaviors of PLA/PBAT blends were investigated using a strain-controlled rheometer (ARES). Samples were tested using a parallel-plate geometry (d = 25 mm) operated at 170 °C. A dynamic frequency sweep test was performed to determine the dynamic properties of the blends. The strain and frequency range used during test was 5 % and 0.1–200 rad/s respectively.

Evaluation of the Reactivity of ESA with PLA and PBAT

PLA and PBAT were extruded respectively with different ESA contents. The extruded pure PLA and PBAT without

ESA were taken as reference. The intrinsic viscosity of these extruded samples was measured and the results are shown in Table 1. Intrinsic viscosity of the pure PLA is decreased from 1.60 to 1.31 dl/g and that of the pure PBAT is only decreased from 1.35 to 1.33 dl/g after extrusion. Obviously, PLA is prone to thermal degradation while PBAT has better thermal stability. However, when ESA is added during extrusion, the intrinsic viscosity of PLA could be basically hold steady. This result implies that the intermolecular chain-extending reaction between ESA and PLA has taken place. For the thermal decomposition of PLA, the ester bond (–CO–O-) is the most likely site for chain scission and that cleavage of this bond would in situ produce the hydroxyl radical and the carboxyl radical. So epoxy groups on ESA could easily react with these radicals thereby reconnects the fractures of molecular chains of PLA [23, 24]. On the other hand, as shown in Table 1, there is no notable viscosity change of PBAT with or without ESA during extrusion. So it can be considered that there is no evident reaction between ESA and PBAT during thermal processing and ESA is mainly a chain extender for the PLA matrix of PLA/PBAT blends.

Mechanical Properties of PLA/PBAT Blend in the Presence of ESA

Various PLA/PBAT blends were prepared by twin-screw extrusion. ESA was used as reactive agent premixed with PLA and PBAT pellets before extrusion. Impact properties and tensile properties of these blends were investigated and the results are shown in Figs. 1 and 2.

Figure 1 shows the effect of PBAT and ESA on impact strength of PLA. In the absence of ESA, the impact strength of pure PLA decreases significantly after undergoing thermal extrusion and that of PLA/PBAT blends increases with increasing PBAT contents. In agreement with early reports [25], in the case of blending PBAT as viscous biodegradable polymer into PLA, the toughness of PLA is clearly improved by PBAT. As shown in Fig. 1, at 15 and 30 wt% of PBAT contents, the impact strength notably increases with the addition of ESA at just 0.1 wt%

Table 1 Influence of ESA on the intrinsic viscosity of PLA and PBAT

ESA content (wt%)	Intrinsic viscosity (dl/g)	
	PLA	PBAT
Pellets	1.60	1.35
0	1.31	1.33
0.3	1.64	1.29
0.5	1.49	1.41
1.0	1.59	1.37
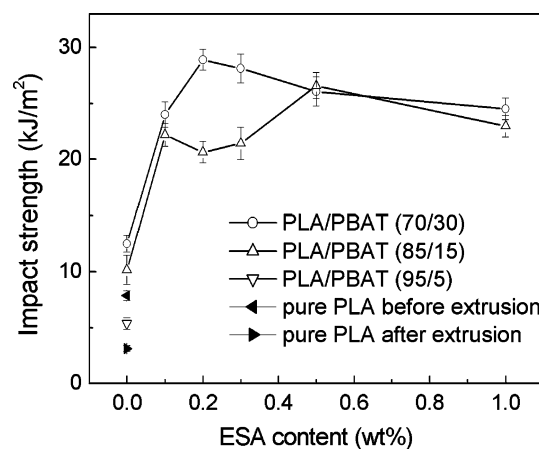
Fig. 1 Impact strength of PLA with different PBAT and ESA contents
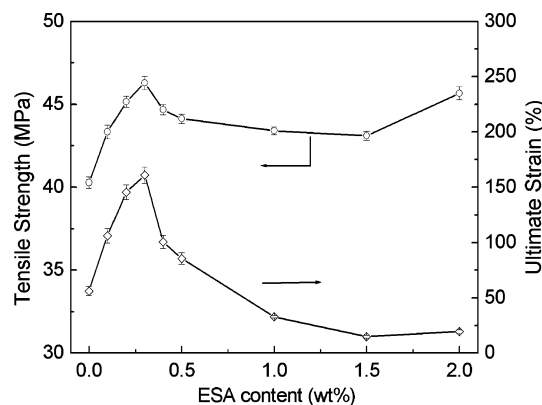
Fig. 2 Ultimate strain and tensile strength of PLA/PBAT (85/15 wt%) blends with different ESA contents

but with further addition of ESA beyond optimum amount range, the impact strength gradually decreases. Increase of impact strength implies that the thermal degradation of PLA during extrusion may be inhibited by just a small quantity of ESA. As mentioned above, epoxy groups can actively react with the free hydroxyl radicals generated by the thermal decomposition of PLA. Thus during processing, including extrusion and injection, ESA repeatedly links the fragments of PLA molecular chains to maintain and even extend the molecular chain. However, excess ESA would not make the impact strength further increase and may even make it decrease. Owing to the multifunctional epoxy structure of ESA, it could be supposed that excessive epoxy groups would lead to some cross-linked structures, which would result in phase separation or heterogeneous distribution in the blend. Considering the significant improvement of impact strength without ESA, 15 wt% PBAT content was chosen for following research.

Figure 2 shows ultimate strain and tensile strength of PLA/PBAT (85/15 wt%) blends with different ESA

contents. As shown in Fig. 2, the ultimate strain of PLA/PBAT (85/15 wt%) blends with ESA, is higher than that without ESA except the ESA contents of beyond 1 wt%. Further addition of ESA beyond the optimum amount has adverse effect on ultimate tensile strain as embrittlement occurs. It may be attributed to the cross-linked structures caused by excessive ESA just like what has happened to impact strength. The ultimate strain of PLA/PCL blend with dicumyl peroxide (DCP) as a initiator also increases first and then drops with the increase of DCP content because of crosslinking [26]. On the other hand, chain extending and possible crosslinking are favorable to maintain the tensile strength, which does not significantly drop after rise (see Fig. 2).

Morphology of the PLA/PBAT Blend with ESA Added

To investigate compatibility of PLA with PBAT, fracture surfaces of tested specimens were observed by using SEM. SEM images of the PLA/PBAT (85/15 wt%) blends with 0 and 0.5 wt% ESA are shown in Fig. 3a, b. Crazing, cavitation, shear banding, crack bridging, and shear yield are identified as important energy dissipation processes involved in the impact fracture of toughened polymer systems [26, 27]. In Fig. 3a, the blend shows a kind of incompatible, namely, two-phase structure with PBAT dispersing evenly in PLA matrix and the cavitation caused by debonding can be clearly identified. As a comparison, in Fig. 3b, with ESA (0.5 wt%) added, the blend shows very little cavitation and much more shear yielding when it is fractured, which is an indication of better compatibility between PLA and PBAT phases. As shown in Fig. 3, the particle size of PBAT remains quite the same. As discussed above, ESA mainly reacts with PLA instead with PBAT. So the improved compatibility of the blend is probably more attributed to the partially branched PLA matrix rather than higher dispersion of PBAT.

Thermal Analysis

DSC curves of PLA/PBAT blends with different ESA contents and pure PBAT are shown in Fig. 4. Each sample was cut from pellets, which underwent rapid cooling after extrusion. So during the first heating scan, cold crystallization and melting of the PLA matrixes can be observed on each curve. However, there is something different in the crystallization behavior of the blends with and without ESA added. Comparing curves in Fig. 4b–e with that in Fig. 4a, the incorporation of ESA increases the cold crystallization temperature (T_c, Table 2) but decreases the crystallization enthalpy and melting enthalpy (ΔH_c and ΔH_m, Table 2). This result implies lowered regularity and depressed activity of PLA chains. Obviously, it should be
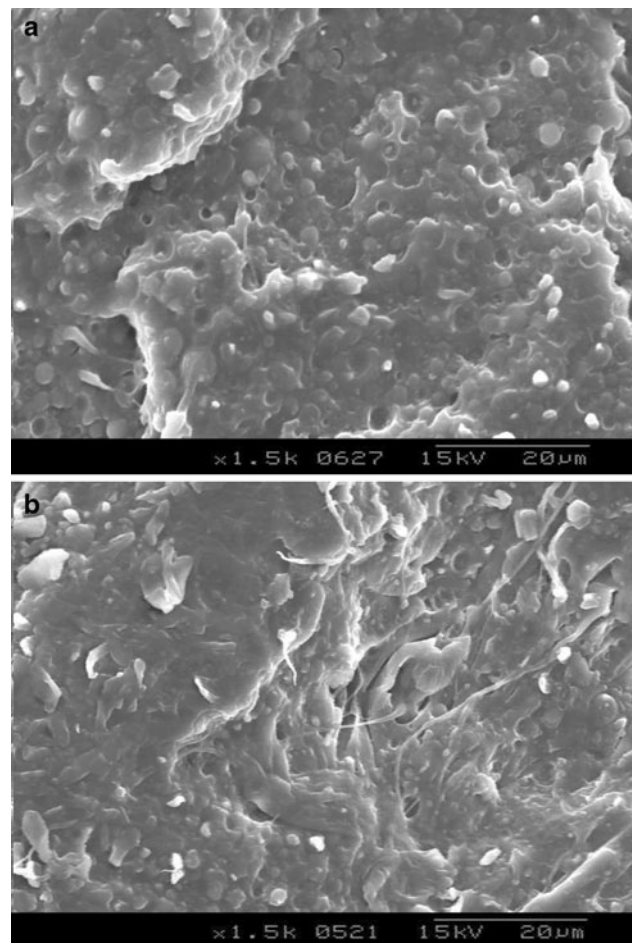

Fig. 3 SEM images of Charpy-fractured surface of the blend. **a** PLA/PBAT blend without ESA added. **b** PLA/PBAT blend with ESA added (0.5 wt%)

attributed to the reaction between PLA and multifunctional ESA.

On the other hand, there are still two glass transitions for each blend (about −25 °C for PBAT phase and about 60 °C for PLA phase) [28]. This result implies that the PLA/PBAT blend is still a two-phase system despite the facts that mechanical properties of blend are efficiently improved and the fracture style has changed to gliding fracture by addition of ESA.

Melt Properties of PLA/PBAT Blends in the Presence of ESA

Polymer processing, especially for blown film, is closely related to melting behavior and rheological properties of polymer materials [29]. In the process of blowing film, higher MS value means better stability and higher strength of the bubble. Therefore, the Melt Index (MI) and Melt Strength (MS) of PLA/PBAT blends with different ESA contents were investigated.
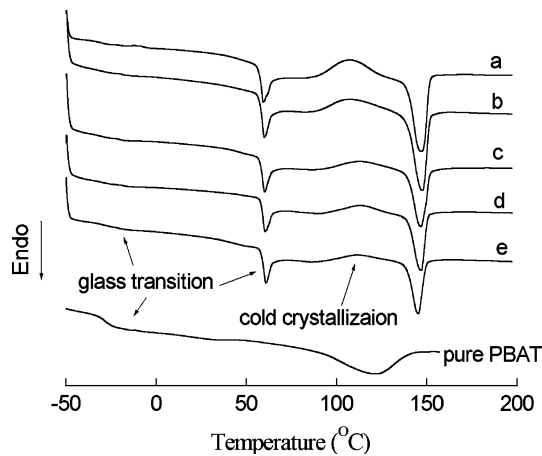
Fig. 4 DSC curves of PLA/PBAT blends with and without ESA added. Heating rate was 10 °C/min. **a** Without ESA; **b** 0.3 wt% ESA; **c** 0.5 wt% ESA; **d** 1.0 wt% ESA; **e** 1.5 wt% ESA

**Table 2** Thermal properties of PLA in blends at different ESA contents

ESA content (wt%)	T_c (°C)	ΔH_c (J/g)	T_m (°C)	ΔH_m (J/g)
0	125.3	7.2	147.4	13.6
0.3	130.0	6.5	147.7	12.9
0.5	134.2	5.0	147.0	10.6
1.0	132.4	5.0	147.1	10.5
1.5	133.5	4.4	145.5	8.8

As shown in Fig. 5, the MI value of PLA/PBAT blends monotonously decreases with the increase of ESA content. Low MI means low fluidity and high melt viscosity. On the other hand, the MS of the blends with increasing ESA contents shows an opposite tendency compared to MI. With the increase of ESA content, the MS of blends monotonously increases. These results show that the reaction between ESA and PLA matrix took place, and the branched structures in PLA and the entanglement in blend were formed.

Rheological Properties of PLA/PBAT Blends with ESA Added

As the addition of ESA results in a finer phase structure (Fig. 3) and effectively increases the ultimate strain and MS of PLA/PBAT blends, its addition also influences the rheological properties of the blends.

G′ and G″ of the blends with different ESA contents are shown in Figs. 6 and 7. It was reported that the incorporation of PBAT had less effect on the G′ and G″ of blend melt at higher frequencies. However, as shown in Figs. 6 and 7, with the addition of ESA, the G′ and G″ of PLA/PBAT blend melts are influenced at nearly all frequencies.
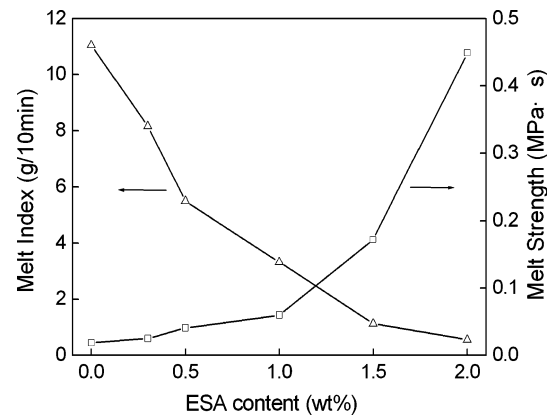

**Fig. 5** Melt index and melt strength of PLA/PBAT with different ESA contents

The melts in the presence of ESA has higher G′ and G″ at all frequencies (except 0.5 wt% content). It indicates that the addition of ESA truly changes the rheological properties of PLA/PBAT blends. In addition, at lower frequencies, the incorporation of 0.5 wt% ESA increases G′ values but has less effect on G″. The higher absolute values of dynamic modulus indicate the formation of entanglement structures in PLA/PBAT melts. PBAT is a copolymer with long polybutylene adipate (PBA) molecular chain segments, so its molecular chains are more flexible than that of plain PLA and are easier to entangle. Now the higher storage modulus (G′) of the melts with the addition of ESA obviously indicates a further increased entanglement density [30].

Based on linear viscoelastic theory, in the terminal zone at low frequency, the curves of narrow M_w distribution of heterogeneous polymer melt can be expressed by power law of $G'(\omega) \propto \omega^2$ and $G''(\omega) \propto \omega$, namely the slopes of $\lg G'(\omega)$ and $\lg G''(\omega)$ curves are 2 and 1 respectively [30–32]. For non-homogeneous polymer blend melt, the slope of $\lg G'(\omega)$ and $\lg G''(\omega)$ curves are expected to be lower than 2 and 1 respectively, and smaller deviation means better compatibility of the blend. The slopes in terminal zone of PLA/PBAT melts from the curves of $G'(\omega)$ and $G''(\omega)$ at lower frequencies ($\omega < 10$ rad/s) are calculated and also presented in Figs. 6 and 7. The slopes of $\lg G'(\omega)$ and $\lg G''(\omega)$ curves for all PLA/PBAT melts are considerably lower and the deviation of the terminal slopes are reduced by addition of ESA at 0.3 and 0.5 wt% contents but enlarged with excessive ESA. The lower slope values and higher absolute values of dynamic modulus indicate the formation of entanglement structures in PLA/PBAT melts. The reduced deviation of the terminal slope indicates improved compatibility of the blend.

The curves of dynamic complex viscosity η^* for PLA/PBAT blends with different ESA contents are presented in Fig. 8. It is clear that the addition of ESA results in much
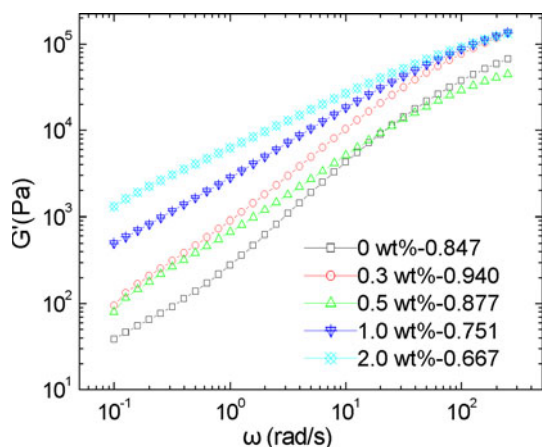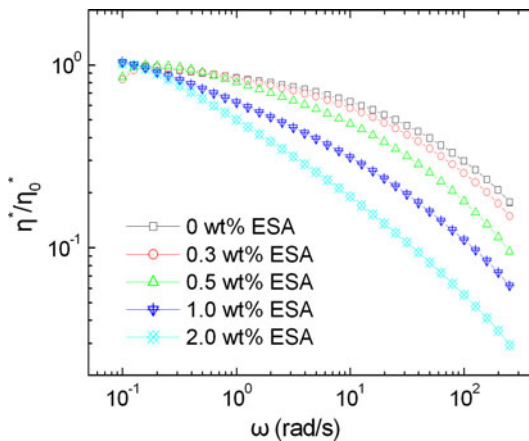
Fig. 6 Frequency dependence of storage moduli G′ (ω) of PLA/PBAT (70/30 wt%) blends with different ESA contents at terminal zone
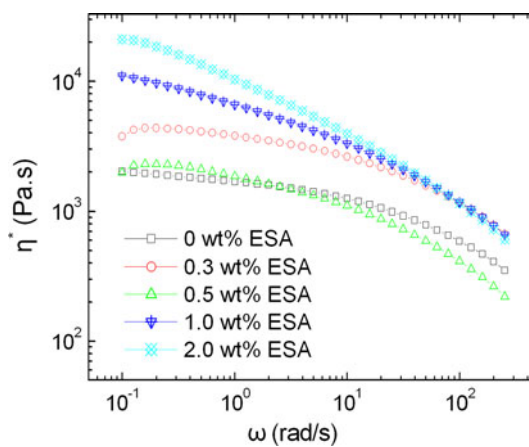
Fig. 8 Frequency dependence of complex viscosity η* of PLA/PBAT (70/30 wt%) blends with different ESA contents
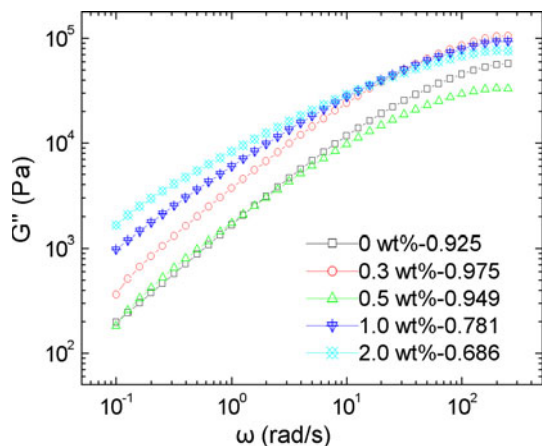
Fig. 7 Frequency dependence of loss moduli G″ (ω) of PLA/PBAT (70/30 wt%) blends with different ESA contents at terminal zone

Fig. 9 Frequency dependence of relative complex viscosity ratio (η*/η₀*) of PLA/PBAT (70/30 wt%) blends with different ESA contents. η_0^* is obtained from Newtonian region

higher η^* at nearly all frequencies, but 0.5 wt% of ESA content is still an exception at higher frequencies. This change indicates that the reaction between ESA and PLA greatly enhances the molecular interactions of the blend system, and the movement of molecular chains is hindered remarkably. On the other hand, the incorporation of ESA has less effect on the expansion of Newtonian region. The relative complex viscosity ratio as a function of frequency is presented in Fig. 9 to investigate the shear-thinning degree of PLA/PBAT blend with different ESA contents [30]. Every sample displays a shear-thinning tendency at frequencies higher than ∼0.2 rad/s and the tendency becomes stronger with the increase of ESA content at the frequency range from 0.2 to 10 rad/s. This result is opposite to what we obtained before [24]. The tendency of shear-thinning becomes weaker with the addition of T-GMA that is a kind of glycidyl methacrylate reactive processing agent with high molecular weight. The increase

of η^* indicates lowered melt fluidity of the blend but the increase of shear-thinning tendency indicates improved melt elasticity of the blend.

Conclusions

The blends of PLA/PBAT with ESA added as reactive agent were prepared by twin screw extrusion. During thermal extrusion, ESA was basically a chain extender for the PLA matrix but had no evident reaction with PBAT. The great improvement in the toughness of PLA based blends could be attributed to the addition of PBAT of no less than 15 wt% and that of ESA of no more than 0.5 wt%. Although SEM micrographs and the reduced deviation of the terminal slope of G′ and G″ could be proofs of better compatibility and adhesion between the two phases, but the blend with ESA was still a two-phase system as indicated

in DSC curves. Rheological results reveal that the addition of ESA increased the storage modulus (G'), loss modulus (G'') and complex viscosity of the blend at nearly all frequencies. The melt strength and melt elasticity of the blend were also improved by addition of ESA.

References

1. Zhang NW, Wang QF, Ren J et al (2007) China Plast Indus 35:62
2. Van de Velde K, Kiekens P (2002) Polym Testing 21:433
3. Lunt J (1998) Polym Degrad Stab 59:145
4. Drumright RE, Gruber PR, Henton DE (2000) Adv Mater 12:1841
5. Ren J, Zhang NW (2004) Mater Rev 18:61
6. Siracusa V, Rocculi P, Romani S et al (2008) Food Sci Technol 19:634
7. Sedlarik V, Saha N, Sedlarikova J et al (2008) Macromol Symp 272:100
8. Auras R, Harte B, Selke S (2004) Macromol Biosci 4:835
9. Witt U, Einig T, Yamamoto M et al (2001) Chemosphere 44:289
10. Gan ZH, Kuwabara K, Yamamoto M et al (2006) J Polym Sci, Part B: Polym Phys 44:3006
11. Jun CL (2000) J Polym Environ 8:33
12. Guan J, Fang Q, Hanna MA (2004) J Polym Environ 12:57
13. Zhang JW, Jiang L, Zhu LY (2006) Biomacromolecules 7:1551
14. Jiang L, Wolcott MP, Zhang J (2006) Biomacromolecules 7:199
15. Jiang L, Liu B, Zhang JW (2009) Ind Eng Chem Res 48:7594
16. Teamsinsungvon A, Ruksakulpiwat Y, Jarukumjorn K (2010) Adv Mater Res 123–125:193
17. Bhatia A, Gupta RK, Bhattacharya SN, Choi HJ (2007) Kor Aust Rheol J 19:125
18. Ma XF, Yu JG, Wang N (2006) J Polym Sci, Part B: Polym Phys 44:94
19. Harada M, Ohya T, Iida K (2007) J Appl Polym Sci 106:1813
20. John J, Bhattacharya M (2000) Polym Int 49:860
21. Wang L, Ma W, Gross RA, McCarthy SP (1998) Polym Degrad Stab 59:161
22. John J, Bhattacharya M (2000) Polym Int 49:860
23. Signori F, Coltelli MB, Bronco S (2009) Polym Degrad Stab 94:74
24. Babanalbandi A, Hill DJT, Hunter DS, Kettle L (1999) Polym Int 48:980
25. Zhang NW, Wang QF, Ren J et al (2009) J Mater Sci 44:250
26. Semba T, Kitagawa K, Ishiaku US et al (2006) J Appl Polym Sci 101:1816
27. Ho K, Kale L, Montgomery S (2002) J Appl Polym Sci 85:1408
28. Ahmed J, Zhang JX, Song Z, Varshney SK (2009) J Therm Anal Calorim 95:957
29. Gu SY, Zhang K, Ren J et al (2008) Carbohydr Polym 74:79
30. Sinha Ray S, Okamoto M (2003) Macromol Mater Eng 288:936
31. Sinha Ray S, Yamada K, Okamoto M, Ueda K (2003) Polymer 44:857
32. Hyun YH, Lim ST, Choi HJ et al (2001) Macromolecules 34:8084